ISSN 1674-1056
http://cpb.iphy.ac.cn
http://iopscience.iop.org/cpb
中国物理 B
Chinese Physics
中国物理 Chinese Physics B

Semiconductor-metal transition in GaAs nanowires under high pressure

Yi-Lan Liang(梁艺蓝), Zhen Yao(姚震), Xue-Tong Yin(殷雪彤), Peng Wang(王鹏), Li-Xia Li(李利霞), Dong Pan(潘东), Hai-Yan Li(李海燕), Quan-Jun Li(李全军), Bing-Bing Liu(刘冰冰), Jian-Hua Zhao(赵建华)

Citation: Chin. Phys. B . 2019, 28(7): 076401. **doi:** 10.1088/1674-1056/28/7/076401
Journal homepage: http://cpb.iphy.ac.cn; http://iopscience.iop.org/cpb

What follows is a list of articles you may be interested in

Pressure-induced isostructural phase transition in α-$Ni(OH)_2$ nanowires

Xin Ma(马鑫), Zhi-Hui Li(李志慧), Xiao-Ling Jing(荆晓玲), Hong-Kai Gu(顾宏凯), Hui Tian(田辉), Qing Dong(董青), Peng Wang(王鹏), Ran Liu(刘然), Bo Liu(刘波), Quan-Jun Li(李全军), Zhen Yao(姚震), Bing-Bing Liu(刘冰冰)
Chin. Phys. B . 2019, 28(6): 066402. **doi:** 10.1088/1674-1056/28/6/066402

Variational and diffusion Monte Carlo simulations of a hydrogen molecular ion in a spherical box

Xuehui Xiao(肖学会), Kuo Bao(包括), Youchun Wang(王友春), Hui Xie(谢慧), Defang Duan(段德芳), Fubo Tian(田夫波), Tian Cui(崔田)
Chin. Phys. B . 2019, 28(5): 056401. **doi:** 10.1088/1674-1056/28/5/056401

Equation of state of $LiCoO_2$ under 30 GPa pressure

Yong-Qing Hu(户永清), Lun Xiong(熊伦), Xing-Quan Liu(刘兴泉), Hong-Yuan Zhao(赵红远), Guang-Tao Liu(刘广涛), Li-Gang Bai(白利刚), Wei-Ran Cui(崔巍然), Yu Gong(宫宇), Xiao-Dong Li(李晓东)
Chin. Phys. B . 2019, 28(1): 016402. **doi:** 10.1088/1674-1056/28/1/016402

The effect of dislocations on the thermodynamic properties of Ta single crystal under high pressure by molecular dynamics simulation

Yalin Li(李亚林), Jun Cai(蔡军), Dan Mo(莫丹), Yandong Wang(王沿东)
Chin. Phys. B . 2018, 27(8): 086401. **doi:** 10.1088/1674-1056/27/8/086401

Transport properties of mixing conduction in CaF_2 nanocrystals under high pressure

Ting-Jing Hu(胡廷静), Xiao-Yan Cui(崔晓岩), Jing-Shu Wang(王婧姝), Jun-Kai Zhang(张俊凯), Xue-Fei Li(李雪飞), Jing-Hai Yang(杨景海), Chun-Xiao Gao(高春晓)
Chin. Phys. B . 2018, 27(1): 016401. **doi:** 10.1088/1674-1056/27/1/016401

Semiconductor–metal transition in GaAs nanowires under high pressure*

Yi-Lan Liang(梁艺蓝)[1,†], Zhen Yao(姚震)[1,†], Xue-Tong Yin(殷雪彤)[1], Peng Wang(王鹏)[1,‡], Li-Xia Li(李利霞)[2], Dong Pan(潘东)[2,§], Hai-Yan Li(李海燕)[1], Quan-Jun Li(李全军)[1], Bing-Bing Liu(刘冰冰)[1], and Jian-Hua Zhao(赵建华)[2]

[1] *State Key Laboratory of Superhard Materials, Jilin University, Changchun* 130012, *China*

[2] *State Key Laboratory of Superlattices and Microstructures, Institute of Semiconductors, Chinese Academy of Sciences, Beijing* 100083, *China*

(Received 18 February 2019; revised manuscript received 6 April 2019; published online 31 May 2019)

We investigate the structural phase transitions and electronic properties of GaAs nanowires under high pressure by using synchrotron x-ray diffraction and infrared reflectance spectroscopy methods up to 26.2 GPa at room temperature. The zinc-blende to orthorhombic phase transition was observed at around 20.0 GPa. In the same pressure range, pressure-induced metallization of GaAs nanowires was confirmed by infrared reflectance spectra. The metallization originates from the zinc-blende to orthorhombic phase transition. Decompression results demonstrated that the phase transition from zinc-blende to orthorhombic and the pressure-induced metallization are reversible. Compared to bulk materials, GaAs nanowires show larger bulk modulus and enhanced transition pressure due to the size effects and high surface energy.

Keywords: GaAs nanowires, high pressure, structural transition, x-ray diffraction

PACS: 64.70.Nd, 91.60.Gf, 63.22.Gh, 61.05.cp **DOI:** 10.1088/1674-1056/28/7/076401

1. Introduction

Gallium arsenide (GaAs) is an important III–V compound semiconductor and provides advantages in high-speed electronic and optoelectronic devices thanks to the direct bandgap and outstanding electron transport properties.[1–3] In the past two decades, GaAs nanowires (NWs) have become a hot topic in nanoscience and nanotechnology with the progress of synthesis methods.[4–6] Due to the small diameter, large surface to volume ratio, highly anisotropic shape, and especially the capability of coupling with integrated silicon circuits, GaAs NWs show unique properties and have novel applications in optoelectronics and nanoscale lasering devices.[7–11] The mechanical and electronic properties are critical for the performance of GaAs NWs devices and have attracted intensive scientific interest. Remarkable elasticity and stiffness have been found in GaAs NWs with elastic strain limit round 11%.[12–14] The electron mobilities of GaAs NWs vary in the range from 1500 $cm^2 \cdot V^{-1} \cdot s^{-1}$ to 3000 $cm^2 \cdot V^{-1} \cdot s^{-1}$ depending on the surface quality and the ballistic transport effect is found to be strongly affected by the stacking faults and impurities of NWs.[15,16] By now, the modification methods for mechanical and electronic properties of GaAs NWs are mainly focused on the improvement on NWs quality which is limited by the state of the art in synthesis methods.

As a fundamental thermodynamic variable, pressure can directly and efficiently reduce interatomic distances and change electronic orbitals and bonding patterns. High-pressure techniques have been widely used to search for new structures and modify the physical properties.[17–20] Under pressure up to 12 GPa, the zinc-blende (ZB) phase GaAs begins to transform into an orthorhombic (OR) phase.[21] The OR phase of GaAs was demonstrated to have the *Cmcm* symmetry and predicted as a metallic phase because the energy bands cross the Fermi level during the phase transition.[22,23] In 2016, Wu *et al.* observed the semiconductor–metal phase transition in GaAs at 12 GPa by *in situ* alternating-current (AC) impedance spectroscopy and temperature dependent electrical resistivity measurements.[24] For the GaAs NWs, high pressure studies have been focused on NWs with diameter from 80 nm to 150 nm, and the irreversible phase transition to OR structure was observed around 19 GPa in both ZB and wurtzite (WZ) NWs.[25,26] It is noticeable that the mechanical properties of GaAs NWs show significant size-dependent effects, especially with diameters down to a few tens of nanometers.[12–14] So it is expected that we will observe unique high-pressure behaviors in GaAs NWs with smaller diameters. The small size and high density surface state of GaAs NWs increase the technical difficulties in electrical resistivity measurements under high pressure, and there is still no report about the metallicity of GaAs NWs under high pressure.

In this work, we investigate the high-pressure behav-

*Project supported by the National Key R&D Program of China (Grant No. 2018YFA0305900), the National Natural Science Foundation of China (Grant No. 11604116), Beijing Municipal Natural Science Foundation, China (Grant No. 1192017), and Youth Innovation Promotion Association, Chinese Academy of Sciences (Grant No. 2017156).

†These authors contributed equally to this work.

‡Corresponding author. E-mail: wangpengtrrs@jlu.edu.cn

§Corresponding author. E-mail: pandong@semi.ac.cn

© 2019 Chinese Physical Society and IOP Publishing Ltd

iors of GaAs NWs with diameter around 40 nm by using synchrotron x-ray diffraction (XRD) and *in-situ* infrared reflectance (IRR) spectroscopy methods up to 26.2 GPa at room temperature. The reversible phase transition from ZB structure to OR structure was observed in GaAs NWs at around 20 GPa. In the same pressure range, a dramatic increase of infrared reflectance indicated the metallization of GaAs NWs.

2. Experimental details

The GaAs NWs under investigation were grown by a solid source molecular-beam epitaxy (MBE) system (VG 80) in a self-catalyzed growth manner. Commercial p-type Si (111) wafers were used as the substrates. Before being loaded into the MBE chamber, the Si substrates were pretreated by chemical etching. At first, we removed the native oxidized layer completely using a HF solution (5%). Then, the substrate was coated with a new oxidized layer by dipping the Si substrate in a solution of H_2SO_4 (98%) and H_2O_2 (30%) (volume ratio $= 4 : 1$).[27] The growth of NWs was commenced by opening the gallium source shutter for 8 s, and then opening the arsenic source shutter at a temperature of 590 ℃. The V/III beam equivalent pressure ratio was 7.3 and the growth time was 50 min.

The morphology and crystal structure of GaAs NWs were characterized by scanning electron microscopy (SEM, Nova NanoSEM 650) and synchrotron XRD. The XRD data were collected with a wavelength of 0.6199 Å at the BL15U1 beam line of Shanghai Synchrotron Radiation Facility (SSRF) at room temperature. The average diameter of the GaAs NWs is about 40 nm and the average length is 4 μm according to the SEM image shown in Fig. 1(a). There is a typical diffraction pattern of ZB structure as shown in Fig. 1(b).

High pressure experiments were carried out at room temperature with a diamond anvil cell (DAC). The pressure was measured by the fluorescence shift of ruby. The IRR spectroscopy measurements were performed with a Bruker Vertex 80 V FT-IR spectrometer equipped with a nitrogen-cooled mercury cadmium telluride (MCT) detector. The GaAs NWs were directly attached to a culet surface of the diamond anvil without pressure transmitting medium. The diameter of the diamond culet was 380 μm and the sample chamber of drilled steel gasket was about 120 μm in diameter and 45 μm in thickness. The reflection spectra were measured at the interface between the sample and diamond anvil. Spectra taken at the internal diamond–air interface of the empty cell were used as the reference for normalizing the sample spectra. We applied additional normalization procedures to consider variations in source intensity. All of the reflectivity spectra that are reported in this paper refer to the absolute reflectivity at the diamond–sample interface. The high-pressure synchrotron XRD experiments were performed at beam line 4w2, Beijing Synchrotron Radiation Facility (BSRF, $\lambda = 0.6199$ Å). The collected two-dimensional diffraction patterns were analyzed by integrating the two-dimensional image with the FIT2D software. For the XRD experiments, the diamond culet diameter was 400 μm and the sample chambers of drilled steel gasket were about 130 μm in diameter and 45 μm in thickness. Methanol–ethanol (4 : 1) was used as the pressure transmitting medium.

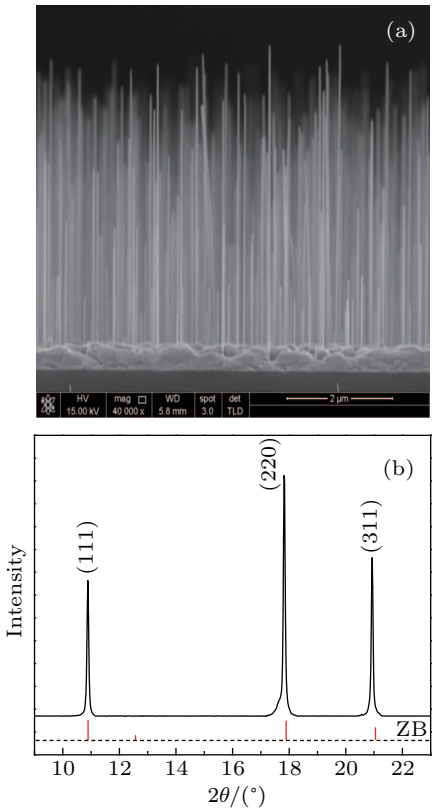


Fig. 1. (a) SEM image of GaAs NWs. (b) XRD patterns of ZB GaAs NWs at ambient pressure.

3. Results and discussion

The XRD patterns of GaAs NWs under high pressure up to 26.2 GPa are presented in Fig. 2(a). In the low pressure range (2.0–19.0 GPa), all the diffraction peaks of ZB phase become broadening and shift to the higher angles with increasing pressure. Up to 20.0 GPa, several diffraction peaks appear at around 14.37°, 14.74°, 15.39°, 20.56°, and 21.19°, which can be indexed to the OR phase.[26] While at the same pressure, the intensity of the diffraction peaks of ZB phase decreases significantly. These results indicate that the phase transition from ZB to OR occurs at 20.0 GPa, which is higher than the transition pressure of bulk GaAs.[21] With the pressure increasing a little bit to 20.9 GPa, all the diffraction peaks of ZB phase disappear, which suggests that the GaAs NWs completely transform into the OR phase. The whole phase transition process accomplishes in a shorter pressure range (20.0–20.9 GPa) comparing with that of bulk GaAs.[21] Then, the OR phase remains stable up to 26.2 GPa, as all the diffraction peaks of OR phase can be observed without any new diffraction peaks.

The evolution of the XRD patterns of GaAs NWs in decompression process is shown in Fig. 2(b). All the diffraction peaks of OR phase remain down to 7.7 GPa and the (311) diffraction peak of ZB phase appears indicating the phase transition from OR to ZB. With further decreasing pressure to 1.7 GPa, all the diffraction peaks of OR phase disappear and only the diffraction peaks of ZB phase can be observed. These results suggest that GaAs NWs transform to the initial ZB phase in the depressurizing process. Comparing with the compression process, the OR–ZB transition in GaAs NWs shows $\sim$ 13 GPa hysteresis in transition pressure. For the pressure-induced reversible phase transition with evident volume collapse, the converse transition can be observed at lower pressure. The ZB–OR transition in GaAs is a first-order phase transition with large volume collapse and the similar hysteretic OR–ZB transition process upon decompression has already been observed in bulk GaAs.[22,23]

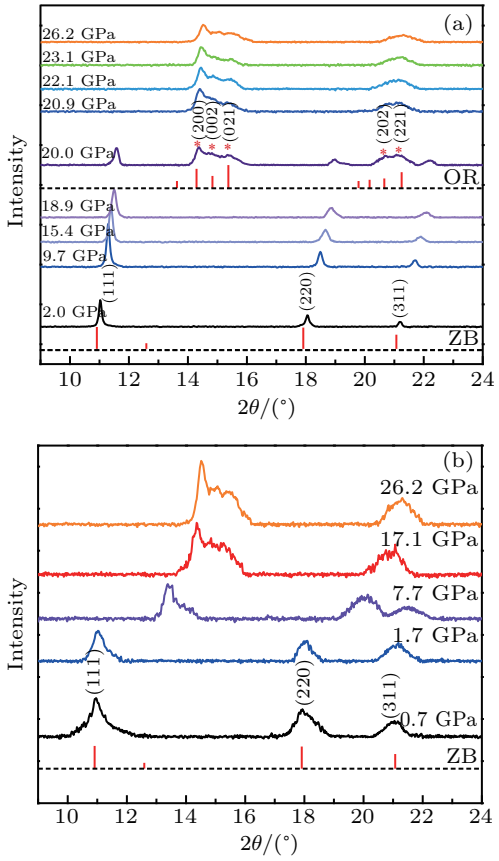


Fig. 2. (a) Synchrotron XRD patterns of GaAs NWs upon compression from 2.0 GPa to 26.2 GPa. Asterisks in the pattern measured at 20.0 GPa represent the diffraction peaks belonging to OR phase, ticks of OR phase are assigned at 23 GPa (Ref. [26]). (b) Synchrotron XRD patterns of GaAs NWs upon decompression from 26.2 GPa to 0.7 GPa.

While high pressure studies have focused on GaAs NWs with larger diameters (80–150 nm), the phase transition from ZB to OR was suggested irreversible. We believe that the reversibility of phase transition is mainly affected by the mechanical properties of the NWs with different diameters, for the size effect on the mechanical properties of GaAs NWs has been demonstrated in previous works.[12–14] The special high pressure behaviors of GaAs NWs in this work could be attributed to the super elasticity and reversible plasticity observed in GaAs NWs with diameters in the range of 50–60 nm.[28]

The cell volumes were determined by Rietveld refinement of XRD patterns using GSAS software package and the cell volumes at various pressures are shown in Table 1. Figure 3 shows the pressure–volume diagram of GaAs NWs. The cell volume of GaAs NWs at ambition pressure is 182(3.6) Å^3. At 20.0 GPa, the corresponding volume change is $\sim$ 16.5%. The experimental data of GaAs MWs were fitted to the third order Birch–Murnaghan equation of state (EOS)

$$P = \frac{3B_0}{2}\left[\left(\frac{V}{V_0}\right)^{-7/3} - \left(\frac{V}{V_0}\right)^{-5/3}\right] \times \left\{1 + \frac{3}{4}(B_0' - 4)\left[\left(\frac{V}{V_0}\right)^{-2/3} - 1\right]\right\},$$

where P and V are the applied pressure and the cell volume under pressure P, respectively. B_0 and B_0' are the bulk modulus and its first pressure derivative. The bulk modulus of GaAs NWs was calculated by fitting the Birch–Murnaghan EOS with different B_0' as shown in Table 2. B_0' was fixed as 3.6, 4.0, 4.4, and 4.8, respectively, and the value of B_0 gradually increases when B_0' decreases. When B_0' was not fixed, the

Table 1. The cell volumes of ZB GaAs NWs at various pressures.

P/GPa	V/Å^3
0	182(3.6)
2.2	175(4.4)
5.8	168 (3.0)
9.7	164(4.5)
13.9	160(4.3)
15.4	159(2.9)
18.0	156(5.9)
19.0	154(2.3)
20.0	151(5.7)

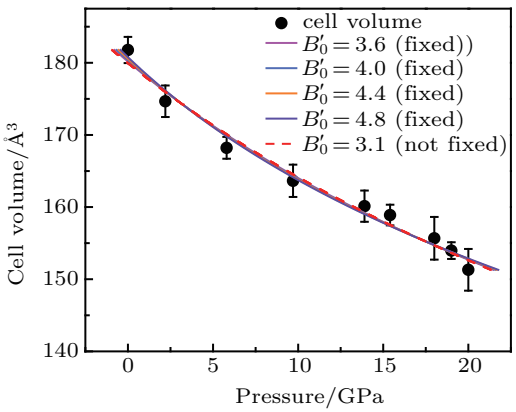


Fig. 3. Pressure–volume diagram of GaAs NWs. The black-solid circles represent the experimental data. The various color solid lines are the fitting results generated via the third-order Birch–Murnaghan equation of state with different fixed B_0', and the red-dashed line is the fitting results without fixed B_0'.

calculated B_0 is 94.4(20.2) GPa with $B_0' = 3.1$. Considering both fixed and unfixed results, the B_0 of GaAs NWs is larger than that of bulk GaAs (75.4 GPa).[22]

Table 2. The bulk modulus B_0 of ZB GaAs with fixed or unfixed B_0'.

B_0'	3.6 (fixed)	4.0 (fixed)	4.4 (fixed)	4.8 (fixed)	3.1 (not fixed)
B_0/GPa	89.9(6.7)	86.3(6.8)	82.9(6.9)	79.6(7.1)	94.4(20.2)

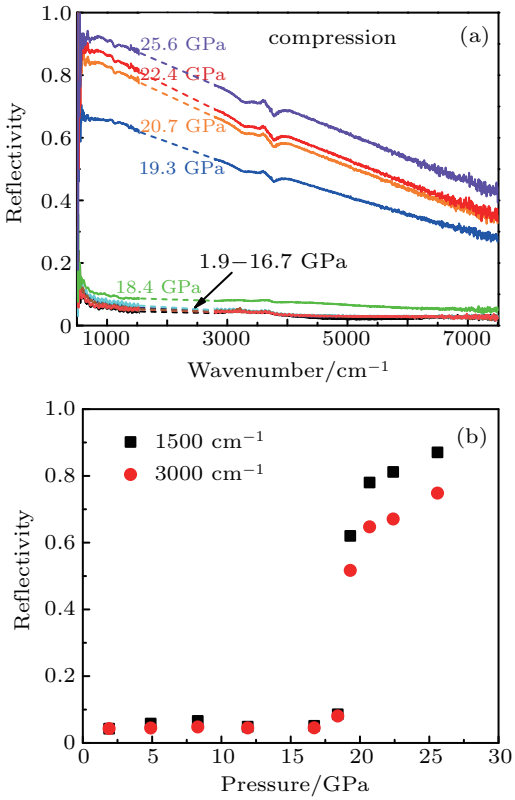


Fig. 4. (a) IRR spectra of GaAs NWs up to 25.6 GPa. (b) Pressure–reflectivity diagram of two different wavenumbers (1500 cm^{-1} and 3000 cm^{-1}) upon compression.

To investigate the electronic properties of GaAs NWs under high pressure, *in-situ* IRR spectroscopy measurements were performed. Figure 4(a) shows the reflectivity spectra with pressure up to 25.6 GPa and the data between 1550 cm^{-1} and 2700 cm^{-1} were cut out from the spectra due to the absorption of diamond. In the pressure range of 1.9–16.7 GPa, there is almost no change of reflectivity. At 18.4 GPa, the reflectivity increases slightly. With the pressure further increasing to 19.3 GPa, a dramatic increase of reflectivity can be observed. Above 20.7 GPa, the reflectivity increases gradually. As shown in Fig. 4(b), the pressure dependence of reflectivity at low frequencies gives the electronic evolution under pressure, and higher reflectivity indicates higher carrier density in the measured samples.[29] Below 18.4 GPa, the reflectivity shows an independent behavior with pressure, suggesting no evident increase of carrier density. The sharp increase of reflectivity can be observed at around 19.3 GPa, indicating the pressure-induced metallization of GaAs NWs. The metallicity of GaAs NWs can be further improved continually with pressure up to 25.6 GPa. The similar transition processes confirm that metallization originates from the phase transition (ZB to OR), which is consistent with the previous reports about bulk GaAs.[22–24]

The reflectivity spectra of GaAs NWs in decompression process are shown in Fig. 5(a). The reflectivity changes gradually in the pressure range of 17.3–25.2 GPa. Below 14.8 GPa, the reflectivity decreases significantly until 8.9 GPa. With further decreasing pressure, the reflectivity changes slightly and recovers back to the initial value. More details can be found in the pressure dependence of reflectivity at low frequencies as shown in Fig. 5(b). The reflectivity spectra of the compression and decompression processes demonstrate pressure-induced reversible metallization in GaAs NWs in agreement with our XRD results.

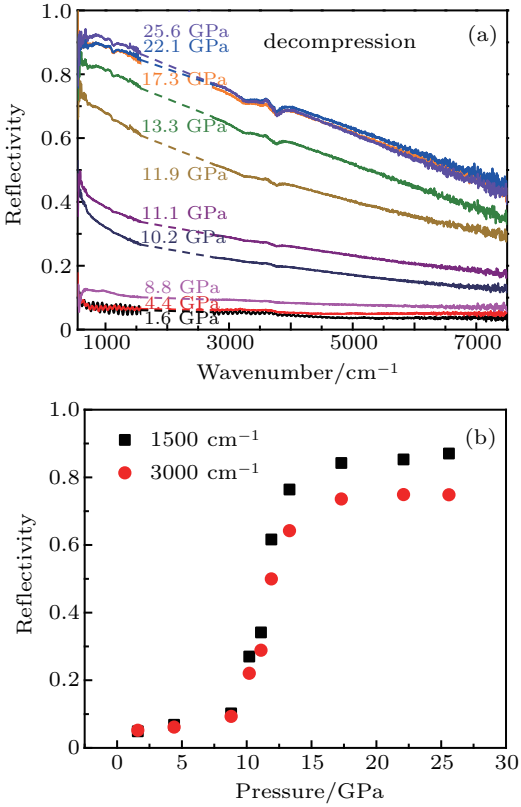


Fig. 5. (a) IRR spectra of GaAs NWs upon decompression at various pressures. (b) Pressure–reflectivity diagram of two different wavenumbers (1500 cm^{-1} and 3000 cm^{-1}) upon decompression.

Due to the high surface to volume ratio and nanosize effects, the GaAs NWs have high surface energy which can affect the optical and mechanical properties, and even the stabilities under high pressure.[18] Enhanced transition pressure with decreasing particle size has been demonstrated in several kinds of nanomaterials mainly due to the surface energy differences.[30–33] It is reasonable that the hysteretic transition pressure of metallization (phase transition from ZB to OR) can be attributed to their high surface energy in GaAs NWs with smaller diameters.

4. Conclusion

In summary, the structural phase transition and electronic properties of GaAs NWs were investigated under high pressure by synchrotron XRD and *in-situ* IRR spectroscopy methods. A pressure-induced reversible phase transition from ZB to OR was observed at around 20.0 GPa. In the same pressure range, pressure-induced reversible metallization of GaAs NWs was confirmed by IRR spectra. The reversibility of phase transition depends on the mechanical properties of GaAs NWs. Compared to bulk materials, GaAs NWs show larger bulk modulus and enhanced transition pressure due to the size effects and high surface energy.

References

[1] Bar-Chaim N, Margalit S, Yariv A and Ury I 1982 *IEEE Trans. Electron. Devices* **29** 1372
[2] Yoon J, Jo S, Chun I S, Jung I, Kim H S , Meitl M, Menard E, Li X, Coleman J J, Paik U and Rogers J A 2010 *Nature* **465** 329
[3] Lee K, Lee J, Mazor B A and Forrest S R 2015 *Light: Sci. & Appl.* **4** e288
[4] Persson A I, Larsson M W, Stenström S, Ohlsson B J, Samuelson L and Wallenberg L R 2004 *Nat. Mater.* **3** 677
[5] Colombo C, Spirkoska D, Frimmer M, Abstreiter G and Fontcuberta i Morral A 2008 *Phys. Rev. B* **77** 155326
[6] Hoang T B, Moses A F, Zhou H L, Dheeraj D L, Fiml, B O and Weman H 2009 *Appl. Phys. Lett.* **94** 133105
[7] Czaban J A, Thompson D A and LaPierre R R 2009 *Nano Lett.* **9** 148
[8] Breuer S, Pfüller C, Flissikowski T, Brandt O, Grahn H T, Geelhaar L and Riechert H 2011 *Nano Lett.* **11** 1276
[9] Saxena D, Mokkapati S, Parkinson P, Jiang N, Gao Q, Tan H H and Jagadish C 2013 *Nat. Photon.* **7** 963
[10] Wang Z and Nabet B 2015 *Nanophotonics* **4** 491
[11] Burgess T, Saxena D, Mokkapati S, Li Z, Hall C R, Davis J A, Wang Y, Smith L M, Fu L, Caroff P, Tan H H and Jagadish C 2016 *Nat. Commun.* **7** 11927
[12] Wang Y B , Wang L F , Joyce H J, Gao Q, Liao X Z , Mai Y W , Tan H H, Zou J, Ringer S P, Gao H J and Jagadish C 2011 *Adv. Mater.* **23** 1356
[13] Paulitschke P, Seltner N, Lebedev A, Lorenz H and Weig E M 2013 *Appl. Phys. Lett.* **103** 261901
[14] Mante P A , Lehmann S, Anttu N, Dick K A and Yartsev A 2016 *Nano Lett.* **16** 4792
[15] Joyce H J, Parkinson P, Jiang N, Docherty C J, Gao Q, Tan H H, Jagadish C, Herz L M and Johnston M B 2014 *Nano Lett.* **14** 5989
[16] Shtrikman H, Popovitz-Biro R, Kretinin A V and Kacman P 2011 *IEEE J. Sel. Top. Quantum Electron.* **17** 922
[17] Hemley R J 2000 *Annu. Rev. Phys. Chem.* **51** 763
[18] San-Miguel A 2006 *Chem. Soc. Rev.* **35** 876
[19] Drozdov A P, Eremets M I, Troyan I A, Ksenofontov V and Shylin S I 2015 *Nature* **525** 73
[20] Zhang L J, Wang Y C, Lv J and Ma Y M 2017 *Nat. Rev. Mater.* **2** 17005
[21] Besson J M, Itié J P, Polian A, Weill G, Mansot J L and Gonzalez J 1991 *Phys. Rev. B* **44** 4214
[22] Samuel T W, Yogesh K V, Craig A V and Arthur L R 1989 *Phys. Rev. B* **39** 1280
[23] Gupta D C and Kulshrestha S 2008 *J. Phys.: Condens. Matter* **20** 255204
[24] Wang J, Wu B J, Zhang G Z, Tian L H, Gu G R and Gao C X 2016 *RSC Adv.* **6** 10144
[25] Zardo I, Yazji S, Marini C, Uccelli E, Fontcuberta i Morral A, Abstreiter G and Postorino P 2012 *ACS Nano* **6** 3284
[26] Zhou W, Chen X J , Zhang J B , Li X H , Wang Y Q and Goncharov A F 2015 *Sci. Rep.* **4** 6472
[27] Li L X, Pan D, Xue Y Z, Wang X L, Lin M L, Su D, Zhang Q L, Yu X Z, So H, Wei D H, Sun B, Tan P H, Pan A L and Zhao J H 2017 *Nano Lett.* **17** 622
[28] Bao P, Wang Y B, Cui X Y, Gao Q, Yen H W , Liu H W, Kong Yeoh W, Liao X Z, Du S, Hoe Tan H, Jagadish C, Zou J, Ringer S P and Zheng R K 2014 *Appl. Phys. Lett.* **104** 021904
[29] Zhang H F, Guan Z, Cheng B Y, Li Q J, Liu R, Zhang J, Liu Z X, Yang K, Cui T and Liu B B 2017 *RSC Adv.* **7** 31597
[30] Wang Z W, Daemen L L, Zhao Y S, Zha C S, Downs R T, Wang X D, Wang Z L and Hemley R J 2005 *Nat. Mater.* **4** 922
[31] He Y, Liu J F, Chen W, Wang Y, Wang H, Zeng Y W, Zhang G Q, Wang L N, Liu J, Hu T D, Hahn H, Gleiter H and Jiang J Z 2005 *Phys. Rev. B* **72** 212102
[32] Wang L H, Liu H Z, Qian J, Yang W G and Zhao Y S 2012 *J. Phys. Chem. C* **116** 2074
[33] Li Q J, Zhang H F, Lin C L, Tian F B, Smith J S, Park C, Liu B B and Shen G Y 2017 *J. Alloys Compd.* **709** 260